Exploiting Polarization Mismatch to Estimate the Orientation of Rotating UHF RFID Tags

Emidio Di Giampaolo, Francesco Martinelli, and Fabrizio Romanelli, *Graduate Student Member, IEEE*

***Abstract*—In this paper we propose a contactless system based on the RFID technology to estimate the rotation of a rotating tagged object. The rotating object is equipped with a linearly polarized RFID tag while the reader is endowed with a circularly polarized antenna. The estimation algorithm exploits the dependence of the phase of the backscattered RFID signal on the relative orientation between the tag's and the reader's antennas. It is based on an Extended Kalman Filter which only uses the phase measurements and assumes an approximate knowledge of the maximum expected torque (i.e., of the maximum rotation acceleration) applied to the object. Numerical and experimental results show that the orientation can be estimated with an error in the order of a few degrees. The maximum allowed rotation speed in online implementations mainly depends on the acquisition rate of the RFID reader, since the EKF-based algorithm can process more than 10^5 phase measurements per s.**

***Index Terms*—UHF RFID, polarization mismatch, angular speed, rotation measurement, extended Kalman filter.**

I. Introduction

THE RADIO Frequency Identification (RFID) technology, originally developed for identification applications, has gained, over the last decade, considerable interest in different application contexts where, in addition to identification, more information is required. With reference to passive RFID in the UHF band, this includes, e.g., functions of sensing and of localization [1], [2]. While localization function resorts to the measure of the strength or the phase of the received signal propagating back from the tag, sensing function can be developed in three different ways (at least) [3]: using a dedicated sensor included in the microchip, using the impedance perturbation of the antenna, and exploiting the variation of propagation parameters.

This last technique is particularly interesting for detecting changes or special phenomena arising in the propagation environment, e.g., medium variation, depolarization, multipath. It consists in measuring the effect of the propagation environment on the RFID signal to estimate changes of properties in the propagation channel [4], [5], [6]. As an example, [7] exploits RFID signals to measure the variations in snow water equivalent (SWE) of a snowpack, [4] exploits depolarization of RFID signal to detect the presence of a scattering body (i.e., a human in a room), [5] uses a multi-baseline approach to detect the effect of multipath in estimating the position of a tag while [6] exploits multipath interferences to detect the vibration of an object near a tag and to measure its vibration frequency. Also the depolarization effect has been used in [8] to estimate the orientation of a tagged object by measuring the RSSI as a function of the relative orientation between linearly polarized reader's and tag's antennas.

In this context a phenomenon affecting the propagation of signals scattered from a moving tag is the changing of the phase induced by the rotation of the tag. That phenomenon arises when the RFID set-up is composed of a circularly polarized reader's antenna and a linearly polarized tag's antenna (i.e., the usual set-up) or vice-versa. In that scenario in fact, there is a dependence of the phase of the backscattered signal on the relative orientation between the tag's antenna and the reader's antenna. To the best of our knowledge that phenomenon has been little investigated in the literature [9]. Nevertheless, it has potentiality to be applied in a number of applications where the dynamic estimate of the orientation or speed rotation of a tagged object is required.

Many industrial applications require the accurate and continuous detection of rotation speed of rotating parts of a machine (e.g., generators, electric motors, machine tool spindles). Besides the use of encoders, there are sensors exploiting technologies based on different physical approaches: optical reflection [10], [11], magnetic field variation [12], [13], electric resonating lumped circuits [14], vibrations [15] to cite a few. An emerging application concerns contactless measurements of wind turbine rotor speed in order to detect future faults with appropriate advance notice. Among different proposed solutions, a method based on video acquisitions at ground level is reported in [16].

Evidently, the exploitation of the changing of phase induced by the rotation of the tag has potentiality to apply also RFID technology in the context of angle and rotation speed measurements. In [9] we studied that phenomenon as a disturb of phase measurements in the context of tag localization by means of a moving vehicle. We analytically characterized that disturb including a more complete model of phase measurements in the framework of localization process based on an

Manuscript received 28 January 2023; revised 3 March 2023; accepted 25 March 2023. Date of publication 30 March 2023; date of current version 19 July 2023. This work was supported in part by the Italian Ministry for Research in the framework of the Program for Research Projects of National Interest (PRIN) under Grant 2017YKXYXJ and Grant 2020RTWES4. *(Corresponding author: Francesco Martinelli.)*

Emidio Di Giampaolo is with the Department of Industrial and Information Engineering and Economics, University of L'Aquila, 67100 L'Aquila, Italy (e-mail: emidio.digiampaolo@univaq.it).

Francesco Martinelli and Fabrizio Romanelli are with the Department of Civil Engineering and Computer Science, University of Rome Tor Vergata, 00133 Rome, Italy (e-mail: francesco.martinelli@uniroma2.it; fabrizio.romanelli@uniroma2.it).

Digital Object Identifier 10.1109/JRFID.2023.3263383

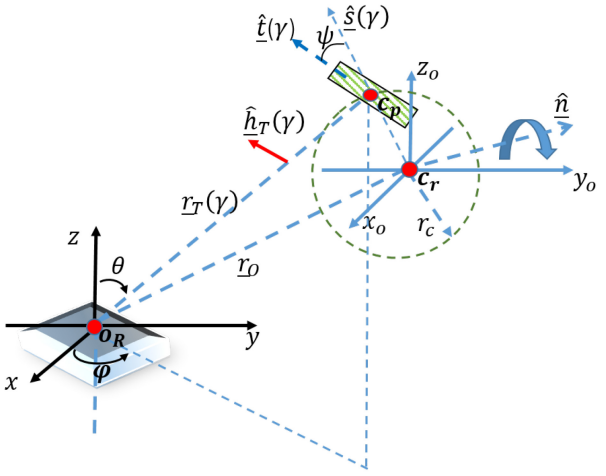

Fig. 1. Geometrical model of the reader-tag link. The fixed reference system (x, y, z) has origin in O_R, the phase center of reader antenna. The rotating tag (dashed green) is fixed on an object (not shown) with reference system (x_o, y_o, z_o). C_r center of rotation, C_p tag's phase center, $\hat{n}$ rotation axis, $\hat{h}_T$ unit vector of the tag's antenna effective height.

Extended Kalman Filter (EKF), demonstrating the improvement in estimating the tag's position. In this work instead, we extend that model with the aim to exploit the phase change for estimating the rotation angle of a tagged object. We define a new scenario where the reader's antenna is fixed in front of a rotating object where a tag is placed on (Figure 1). For the reciprocity the contrary is also possible, i.e., a standing tag in front of a rotating reader's antenna has a similar model. Different geometrical and electrical parameters are defined to account for the uncertainty in the position of the tag with respect to the reader's antenna. A new version of the EKF has been implemented for that estimate while an extensive numerical analysis is reported to show potentialities and limits of the method. Finally, numerical results are compared with experimental measurements to validate the method.

The paper is organized as follows: Section II defines the problem in terms of geometrical and operative parameters, Section III shows the estimation approach while the results of numerical investigation and experimental activity are reported in Sections IV and V, respectively. Section VI discusses the obtained results and draws some conclusions for possible applications.

II. Notation and Problem Formulation

The objective of the method is to estimate the rotation of an object tagged with an RFID tag, only resorting to the measurement of the phase of the backscattered signal. In the following, we denote the symbol of a vector with an underlined variable, the unit vector with a hat underlined variable while a variable defined as a vector without underlining represents the magnitude of that vector. Finally a scalar variable with only a hat represents the estimate of that variable.

A. Backscattering Model

We consider a tagged rotating object in front of a circularly polarized reader's antenna that is shown together with the reference system (x, y, z) in Fig. 1. The tag has a linearly polarized antenna (e.g., dipole-like) and rotates jointly with the object (not shown in Fig. 1) around the axis identified by the unit normal vector $\underline{\hat{n}}$. Let γ be the angle of this rotation. We assume that the rotation of the tag occurs on a plane (that choice represents a recurring situation but also simplifies the description) and define that plane with its unit normal vector $\underline{\hat{n}}$. The distance between the phase center O_R of reader's antenna and the center of rotation C_r is r_0 (it is time invariant), while the distance between C_r and the phase center of the tag's antenna C_p is r_c. So, the phase center C_p describes a circumference of radius r_c during the rotation. The instantaneous position of C_p with respect to O_R is given by the vector $\underline{r}_T$, while the time variant direction between C_r and C_p is described by the unit vector $\underline{\hat{s}}$ (i.e., $\underline{r}_T(\gamma) = \underline{r}_0 + r_c \cdot \underline{\hat{s}}(\gamma)$). The orientation of the tag on the plane of rotation is given by the unit vector $\underline{\hat{t}}$, which forms a constant angle ψ with $\underline{\hat{s}}$. Finally, the direction of the electric field hold by the tag is described with the unit vector of the effective height of tag's antenna, i.e., $\underline{\hat{h}}_T$. All time variant quantities are functions of the rotation angle γ.

The backscattered signal received by the reader is

$$V(\gamma) = V_0(P_{in}, Z_{in}, r_T(\gamma)) \cdot \left(\underline{h}_T(\gamma) \cdot \underline{h}_R\right)^2 e^{-jK_0 2r_T(\gamma)}, \quad (1)$$

where the magnitude V_0 depends on the power P_{in} used to interrogate the tag, on the modulating impedance Z_{in} of the tag and on the magnitude of the position vector $\underline{r}_T$. Vectors $\underline{h}_T(\gamma)$ and $\underline{h}_R(\theta, \phi)$ are the effective heights of tag's and reader's antenna, respectively, while K_0 is the propagation constant.

Since we consider a circularly polarized reader's antenna, the unit vector of its effective height is

$$\underline{\hat{h}}_R(\theta, \phi) = \frac{\underline{\hat{\theta}} + jAR(\theta, \phi)\underline{\hat{\phi}}}{\sqrt{1 + AR^2}}, \quad (2)$$

where $AR(\theta, \phi)$ is the axial ratio that depends on the direction between O_R and C_p, given in terms of spherical coordinates θ and ϕ. Any circularly polarized antenna, in fact, is not perfectly polarized in all directions, but in general its polarization changes from circular to elliptical or linear as a function of the direction.

For tag's antenna, we restrict our interest to dipole-like tags. In that case, the unit vector of the effective height $\underline{\hat{h}}_T(\gamma)$ is orthogonal to $\underline{r}_T$ and lies on the plane described by the couple $(\underline{\hat{r}}_T, \underline{\hat{t}})$. Hence it is given by

$$\underline{\hat{h}}_T(\gamma) = \frac{\underline{\hat{r}}_T \times \underline{\hat{r}}_T \times \underline{\hat{t}}}{\|\underline{\hat{r}}_T \times \underline{\hat{r}}_T \times \underline{\hat{t}}\|} \quad (3)$$

In case of $\underline{\hat{r}}_T \,//\, \underline{\hat{t}}$, $\underline{\hat{h}}_T$ is given by any unit vector orthogonal to $\underline{\hat{r}}_T$.

From (1) we retrieve the phase measured by the reader. It is:

$$\phi = \mod\left(-2K_0 r_T(\gamma) + 2\gamma_p + \phi_0 + n_\phi, \pi\right), \quad (4)$$

where $2K_0 r_T(\gamma)$ accounts for the round trip between the reader's and the tag's antennas, n_ϕ is the measurement error, modeled for simplicity as a 0 mean Gaussian random variable with standard deviation σ_ϕ and ϕ_0 is an unknown phase offset, depending on the specific tag (it also includes the initial

rotation angle γ_0). γ_p instead depends on the instantaneous relative orientation between $\hat{\underline{h}}_T(\gamma)$ and $\hat{\underline{h}}_R$, i.e.,

$$\gamma_p = \arg\left(\hat{\underline{h}}_T(\gamma) \cdot \hat{\underline{h}}_R\right) = \arctan\left(\frac{A}{B}\right), \tag{5}$$

with

$$A = AR(\theta, \phi)\big(\cos(\phi)h_{Ty} - \sin(\phi)h_{Tx}\big)$$
$$B = \cos(\theta)\cos(\phi)h_{Tx} + \cos(\theta)\sin(\phi)h_{Ty} - \sin(\theta)h_{Tz},$$

where $\hat{\underline{h}}_T(\gamma)$ and $\hat{\underline{h}}_R$ are written in terms of the Cartesian components.

B. Estimation Model

Being γ the rotation angle of the tagged object, we denote by $\omega = \dot{\gamma}$ and $\alpha = \ddot{\gamma}$ the angular velocity and acceleration, respectively. Then, the discrete time dynamics of these variables can be described by the following set of equations:

$$\gamma_{k+1} = \gamma_k + \omega_k \delta_T \tag{6}$$
$$\omega_{k+1} = \omega_k + \alpha_k \delta_T \tag{7}$$
$$\alpha_{k+1} = \alpha_k + \tau_k, \tag{8}$$

where the subscript k represents the value of the considered variable at time step k and δ_T is the sampling time. The quantity τ_k is the angular acceleration variation in the last time step. It depends on the torques applied to the rotating object, it is assumed unknown and only a maximum value τ_M for its absolute value is assumed available. The objective is the estimation of γ and ω only using the information coming from the measurements in (4).

In practical applications a number of the geometric parameters defining the backscattering model may be not exactly known, e.g., the distance r_0, the radius of rotation r_c, the angles ψ, θ, ϕ and the plane of rotation $\hat{\underline{n}}$. For this reason, we improve the model by considering these parameters only approximately known, i.e., we assume for them a nominal value subject to an unknown perturbation.

In a likely scenario, the reader's antenna points toward the tag along its maximum gain direction, that we assume to be along $\theta = 0$ in the scheme of Fig. 1. We assume also that $\hat{\underline{n}} \equiv \hat{\underline{z}}$ and $C_r \equiv C_p$. As a consequence, $\hat{\underline{r}}_T \perp \hat{\underline{t}}$, $\hat{\underline{t}} \equiv \hat{\underline{s}}$ and $r_T \equiv r_0 = D$, i.e., the distance between the phase centers is constant. Under these conditions, $\gamma \equiv \phi$ and (5) simplifies into

$$\gamma_p = \text{atan2}(AR\sin(\gamma), \cos(\gamma)). \tag{9}$$

Since a good antenna has its best circular polarization along the direction of maximum gain, we can consider the ideal case $AR = 1$ for $\theta = 0$, so that $\gamma_p \equiv \gamma$.

In that scenario the nominal relative position of the reader with respect to the object is assumed to roughly meet the following requirements:

- the antenna of the reader and the antenna of the tag on the object lay on parallel planes (i.e., $\hat{\underline{n}} \equiv \hat{\underline{z}}$);
- the dipole-like antenna phase center coincides with the rotation axis of the object (i.e., $r_c = 0$);
- the projection of the phase center of the tag antenna on the plane of the reader antenna coincides with the phase center of the reader antenna (i.e., $C_p \equiv (0, 0, D)$);
- the axial ratio is known even though not exactly equal to one.

The problem will be solved under the nominal value of the parameters listed so far, while D will be included in the estimation process: for this reason only a roughly initial value of D will be assumed known. As mentioned, the proposed solution will be tested under some (unknown) perturbations on these parameters to show its robustness.

III. Solution Approach

The solution to the problem defined in Section II is based on an Extended Kalman filter (EKF), where the system state X to be estimated contains the angle γ, the speed ω and the acceleration α of the rotating tag. Also the coordinate D is included among the estimated variables, hence $X = [\gamma, \omega, \alpha, D]^T$.

Let D_n denote the nominal value for D. If we assume a zero initial velocity and if we take the initial angle as reference (i.e., $\gamma_0 = 0$), the initial estimate is given by

$$\hat{X}_0 = [0,\ 0,\ 0,\ D_n]^T. \tag{10}$$

The initial covariance matrix associated with this estimate is assumed diagonal and is given by

$$P_0 = \text{diag}\Big(\Big[0,\ 0,\ \sigma^2_{\alpha,0},\ \sigma^2_D\Big]\Big), \tag{11}$$

where $\sigma_{\alpha,0}$ and σ_D are the standard deviations characterizing the uncertainty in the initial value of α_0 and, respectively, of the coordinate D. If the initial velocity can be different from zero, we can consider this by taking $P_0(2,2) = \sigma^2_{\omega,0}$, where $\sigma_{\omega,0}$ is the standard deviation characterizing the uncertainty in the initial value of the rotation speed ω.

The prediction step of the filter is based on the dynamics reported in (6)-(8), while D presents a constant dynamics given by $D_{k+1} = D_k$ for all k. Hence, if $\hat{X}_k = [\hat{\gamma}_k, \hat{\omega}_k, \hat{\alpha}_k, \hat{D}_k]^T$ denotes the state estimate at time k, the equations of the prediction step of the filter are given by:

$$\hat{\gamma}^-_{k+1} = \hat{\gamma}_k + \hat{\omega}_k \delta_T \tag{12}$$
$$\hat{\omega}^-_{k+1} = \hat{\omega}_k + \hat{\alpha}_k \delta_T \tag{13}$$
$$\hat{\alpha}^-_{k+1} = \hat{\alpha}_k \tag{14}$$
$$\hat{D}^-_{k+1} = \hat{D}_k. \tag{15}$$

Since τ_k in (8) is not known, we consider it as a noise $n_{\tau,k}$. This quantity will be modeled by a 0 mean Gaussian random variable with standard deviation $\sigma_\tau = \tau_M/3$ depending on the maximum expected value τ_M of $|\tau_k|$:

$$n_{\tau,k} \sim \mathcal{N}\Big(0, \sigma^2_\tau\Big). \tag{16}$$

The covariance matrix is updated according to the following equation:

$$P^-_{k+1} = F\,P_k\,F' + Q, \tag{17}$$

where F is the state matrix associated with the linear dynamics of X (in this case it is a 4×4 matrix coincident with an

identity matrix apart from $F(1,2) = F(2,3) = \delta_T$) and Q is a 4×4 matrix with all the elements equal to 0 apart from $Q(3,3) = \sigma_\tau^2$. If D is expected to change during the experiment (e.g., reader manually operated and not positioned on a fixed support), we could take into account of this variation by considering $Q(4,4) = \sigma_{c_D}^2$, being σ_{c_D} the standard deviation of the perturbation characterizing the change of D. In this paper, where D is assumed constant, $Q(4,4) = 0$.

The correction step of the EKF is instead based on the measurement model given by (4), where the various unknown parameters r_{0x}, r_{0y}, r_c and AR are assumed equal to their nominal value ($r_{0x} = r_{0xn}$, $r_{0y} = r_{0yn}$, $r_c = r_{cn}$ and $AR = AR_n \in (0,1)$), which value will be specified in the numerical examples.

First of all we need to express the distance r_T in (4) as a function of the estimated and nominal quantities. We have $r_T = \sqrt{r_{Tx}^2 + r_{Ty}^2 + D^2}$, where $r_{Tx} = r_{0x} + r_c \cos(\gamma)$ and $r_{Ty} = r_{0y} + r_c \sin(\gamma)$ are the coordinates of the center of the tag antenna with respect to the reader antenna. So, in the EKF, we will use for r_T the value obtained using the estimated and nominal values for the different quantities:

$$\hat{r}_{T,k+1}^- = \sqrt{\left(\hat{r}_{Tx,k+1}^-\right)^2 + \left(\hat{r}_{Ty,k+1}^-\right)^2 + \left(\hat{D}_{k+1}^-\right)^2}, \quad (18)$$

where

$$\hat{r}_{Tx,k+1}^- = r_{0xn} + r_{cn} \cos\left(\hat{\gamma}_{k+1}^-\right), \quad (19)$$

$$\hat{r}_{Ty,k+1}^- = r_{0yn} + r_{cn} \sin\left(\hat{\gamma}_{k+1}^-\right). \quad (20)$$

Then, if

$$\hat{\gamma}_{p,k+1}^- = \text{atan2}\left(AR_n \sin\left(\hat{\gamma}_{k+1}^-\right), \cos\left(\hat{\gamma}_{k+1}^-\right)\right)$$

denotes the expected value of γ_p in (9) according to the nominal and estimated quantities, the expected phase measurement is given by

$$\hat{\phi}_{k+1}^- = \quad \text{mod}\left(-2K_0\hat{r}_{T,k+1}^- + 2\hat{\gamma}_{pk+1}^-, \pi\right).$$

In this expression the offset, being unknown, is not included. This is justified by the fact that the effect on the measurements of the offset is very similar to the effect due to a change of D, in such a way that the estimate of D will compensate the effect of the unknown offset. More in detail, the EKF will produce an estimate $\hat{D}$ of the constant parameter D such that $-2K_0\hat{D} = -2K_0 D + \phi_o$.

The innovation at time $k+1$ is given by the difference

$$\Delta\phi = \phi_{k+1} - \hat{\phi}_{k+1}^-,$$

which, being a difference between angles characterized by a periodicity of π radians, will be reported in the interval $(-\pi/2, \pi/2)$.

The correction step of the filter is then given by:

$$\hat{X}_{k+1} = \hat{X}_{k+1}^- + K_{k+1}\,\Delta\Phi, \quad (21)$$

where

$$K_{k+1} = P_{k+1}^- H^T \left(H P_{k+1}^- H^T + \sigma_\phi^2\right)^{-1}$$

is the Kalman gain. In this expression H is the Jacobian matrix of the measurement model (4) with respect to the state and is given by

$$H = [H_1,\ 0,\ 0,\ H_4],$$

with

$$H_1 = -\frac{2K_0 r_{cn}\left(-\hat{r}_{Tx,k+1}^- \sin\left(\hat{\gamma}_{k+1}^-\right) + \hat{r}_{Ty,k+1}^- \cos\left(\hat{\gamma}_{k+1}^-\right)\right)}{\hat{r}_{T,k+1}^-} + \frac{2\,AR_n}{\cos^2\left(\hat{\gamma}_{k+1}^-\right) + AR_n^2 \sin^2\left(\hat{\gamma}_{k+1}^-\right)}$$

and

$$H_4 = -2K_0 \frac{\hat{D}_{k+1}^-}{\hat{r}_{T,k+1}^-}.$$

Finally, the covariance matrix is updated as follows:

$$P_{k+1} = (I - K_{k+1} H) P_{k+1}^-, \quad (22)$$

with I the 4×4 identity matrix.

IV. Numerical Investigation and Examples

The numerical investigation has been performed by considering two different cases: an ideal scenario (Section IV-A) and a perturbed situation (Section IV-B). In the ideal case, all the uncertain parameters take their nominal value and $AR = 1$. In the perturbed scenario, $AR = 0.8$ and all the uncertain parameters are subject to a small perturbation with respect to their nominal value. Finally, in Section IV-C, an extensive numerical analysis is performed to investigate the robustness of the approach with respect to several uncertain parameters of the model.

The signal frequency considered in this paper is $f = 867MHz$ and, unless otherwise specified, the standard deviation σ_ϕ of the noise in the phase measurements will be assumed 10°. The (unknown) acceleration considered in the simulations, comprising $T = 200$ steps, is of the type reported in Fig. 2, with the maximum absolute value $\tau_M \approx 90°/s^2$. As a consequence, we considered $\sigma_\tau = 30°/s^2$ in the Q matrix of the EKF described in Section III, while $\sigma_{\alpha,0}$ in (11) has been taken equal to $60°/s^2$. The sampling time δ_T considered in the simulations is 0.1 s.

The performance considered in all the numerical examples is the mean absolute error in the rotation angle γ estimation. It is given by:

$$e_\gamma = \frac{1}{T}\sum_{k=1}^{T} |\gamma_k - \hat{\gamma}_k|, \quad (23)$$

being $T = 200$ the duration of each simulation.

A. Ideal Scenario

In this section the proposed approach is applied to estimate the rotation angle γ assuming an ideal scenario where $AR = 1$ and all the unknown parameters take their nominal (known) value: $r_{0x} = r_{0xn} = 0$, $r_{0y} = r_{0yn} = 0$, $r_c = r_{cn} = 0$. Also the coordinate $D = D_n = 1$ m will be assumed exactly known

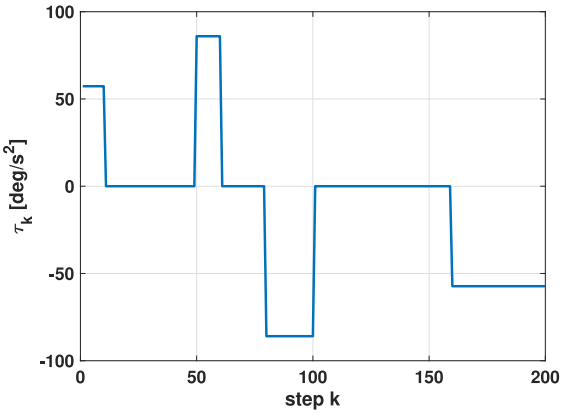

Fig. 2. The rotation acceleration signal τ_k applied to the tagged object in each time step k of the simulations.

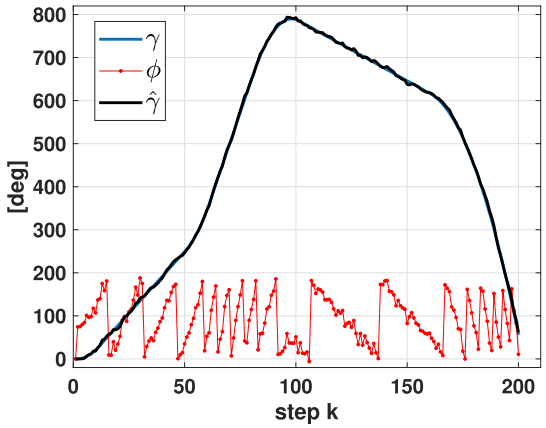

Fig. 3. The algorithm applied in the ideal scenario described in Section IV-A: the rotation angle γ and its estimate $\hat{\gamma}$, almost overlapping, are reported together with the phase measurements. The average estimation error e_γ obtained in this simulation is 2.6°.

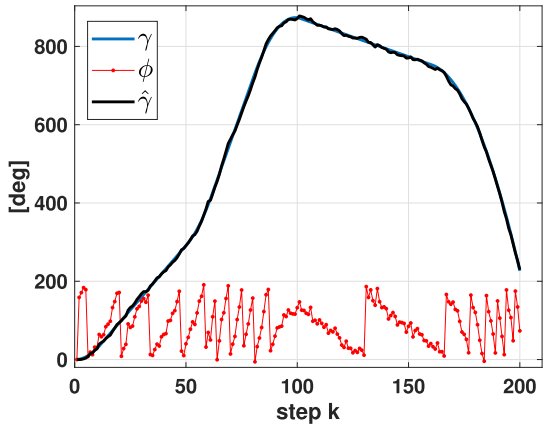

Fig. 4. The algorithm applied in the perturbed scenario described in Section IV-B: the rotation angle γ and its estimate $\hat{\gamma}$ are reported together with the phase measurements. The average estimation error e_γ obtained in this simulation is 3.5°.

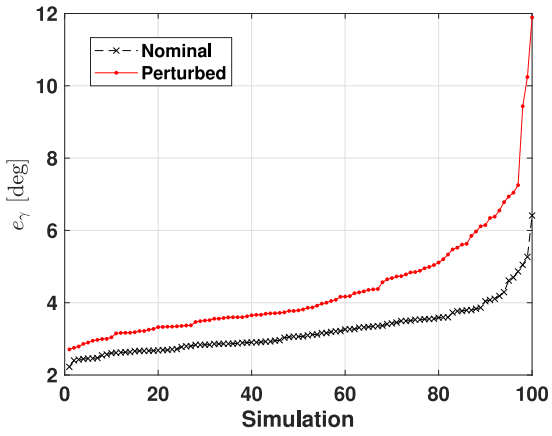

Fig. 5. The estimation error e_γ obtained in 100 independent simulations under the ideal scenario described in Section IV-A and the perturbed situation described in Section IV-B: the errors are plotted from the best to the worst case.

together with the phase offset ϕ_o, assumed 0. The initial tagged object rotation speed ω_0 will be assumed equal to zero and known.

The behavior of the proposed approach in one of the simulations is reported in Fig. 3: it is possible to see how the true rotation angle γ is well estimated with an average error $e_\gamma = 2.6°$. The average estimation error e_γ obtained in 100 independent simulations is reported in Fig. 5 together with the error obtained in 100 simulations under the perturbed scenario described below in Section IV-B.

B. Perturbed Scenario

In this section we consider a perturbed scenario where the nominal AR is assumed equal to 0.8. The true value of AR considered in the simulations is obtained by adding to this nominal value an unknown 0 mean Gaussian random variable with standard deviation 0.05. A similar perturbation is considered for the uncertain parameters r_{0x}, r_{0y} and r_c by adding to their nominal value (assumed 0) a 0 mean Gaussian random variable with standard deviation 0.05 m. The same perturbation is added to the nominal value $D_n = 1$ m of D. The phase offset ϕ_o is now assumed unknown and randomly uniformly sampled from the interval (0, 180°) in each simulation. Finally, an unknown 0 mean Gaussian random variable with standard deviation $10°/s$ is added to the 0 nominal value of the initial rotation speed in each simulation. The EKF is executed in this case using the nominal value of the parameters and by initializing with D_n the estimate of D.

The behavior of the approach is not significantly compromised by these perturbations as reported in Fig. 4, for one of the considered simulations, and in Fig. 5, where the estimation error of 100 independent simulations is compared with the ideal scenario.

C. Robustness Analysis

In this section, a robustness analysis is performed with respect to several uncertain parameters of the model. More in detail, we consider a single specific uncertain parameter at the time and evaluate the performance of the algorithm under increasing perturbations applied to this parameter. All other

TABLE I
AR PERTURBATION EFFECTS

σ_{AR}	0.01	0.02	0.05	0.1
m_{e_γ} [deg]	4.25	4.36	4.54	4.99
σ_{e_γ} [deg]	1.57	1.83	1.81	1.91

TABLE II
r_{0x}, r_{0y} PERTURBATION EFFECTS

$\sigma_{r_{0x,y}}$ [m]	0.01	0.05	0.1	0.2
m_{e_γ} [deg]	3.73	4.41	5.95	9.28*
σ_{e_γ} [deg]	0.87	1.83	3.86	8.76*

TABLE III
r_c PERTURBATION EFFECTS

σ_{r_c} [m]	0.01	0.05	0.1	0.2
m_{e_γ} [deg]	3.73	4.47	6	9.54*
σ_{e_γ} [deg]	0.88	1.65	3.68	8.46*

parameters in the simulation are like in Section IV-B, that is, all other parameters are characterized by the small perturbation described in that section.

We report, respectively, in Tables I, II and III, the effect of different perturbations on the uncertain parameters *AR*, r_{0x}, r_{0y} and r_c. We also analyze the effect of the uncertainty in the knowledge of coordinate D (Table IV) and the effect of a stronger noise n_ϕ in the phase measurements (Table V).

Each table reports, for each different size of the perturbation considered, the mean m_{e_γ} and the standard deviation σ_{e_γ} (both in deg) of the estimation error e_γ obtained in 1000 independent simulations. The perturbation is a 0 mean Gaussian random variable with the standard deviation σ reported in the first line of the tables (e.g., σ is σ_{AR} in Table I), added to the considered parameter (while all other parameters are like in Section IV-B).

Based on the results reported in Table I, it is possible to observe how an increase in the perturbation on parameter *AR* does not significantly degrade the performance of the algorithm. In each one of the 1000 simulations, the true value of *AR* is generated according to $0.8+n_{AR}$, being $n_{AR} \sim \mathcal{N}(0, \sigma_{AR})$ a 0 mean Gaussian random variable with standard deviation σ_{AR}. The algorithm always runs with the nominal value $AR = 0.8$.

The effect of the perturbation on r_{0x} and r_{0y} (Table II) is similar to the one on r_c (Table III). It is not very significant if the standard deviation of the perturbation is not too large, namely, if it is not larger than 0.1 m, which corresponds to the first three values of σ reported in Tables II and III. On the contrary, for $\sigma = 0.2$ m, in both cases we observed some outliers: the * in the tables means that the average value m_{e_γ} and the standard deviation σ_{e_γ} have been computed in this case by removing some outliers. An outlier is an estimation error e_γ larger than 200 deg, which usually corresponds to a divergence in the estimate produced by the EKF. In Table II, for $\sigma_{r0x,y} = 0.2$ m, we observed only one outlier (over 1000 simulations), while we observed four outliers (out of 1000 simulations) for $\sigma_{r_c} = 0.2$ m in Table III. As for Table II, we have added a perturbation on both r_{0x} and r_{0y} parameters (i.e., in each simulation, $r_{0x} \sim \mathcal{N}(0, \sigma_{r_{0xy}})$ and $r_{0y} \sim \mathcal{N}(0, \sigma_{r_{0xy}})$, while the EKF used the nominal values $r_{0x} = r_{0y} = 0$). In Table III, we considered in each simulation $r_c \sim \mathcal{N}(0, \sigma_c)$, while the EKF used the nominal value $r_c = 0$. The presence of outliers depends on the fact that the algorithm is designed to deal with small perturbations on the unknown motion parameters. To handle larger perturbations on r_{0x}, r_{0y} and r_c (or, in general, if the tagged object is expected to perform a more complex motion significantly different from a rotation around the center of its tag's antenna), it would be necessary to set up a different Kalman Filter which also introduces the estimation of the unknown motion parameters. However this would increase the computational complexity of the filter and would deteriorate its convergence properties.

TABLE IV
D PERTURBATION EFFECTS

σ_D [m]	0.01	0.05	0.1	0.2	0.5
m_{e_γ} [deg]	4.47	4.47	4.57	4.65	5.11
σ_{e_γ} [deg]	1.85	1.69	1.86	1.82	3.73

TABLE V
σ_ϕ PERTURBATION EFFECTS

σ_ϕ [deg]	5^o	10^o	15^o	20^o
m_{e_γ} [deg]	3.28	4.51	5.81	10.13*
σ_{e_γ} [deg]	1.78	1.82	3.92	16.33*

As shown in Table IV, the uncertainty in the knowledge of the D coordinate does not significantly affect the behavior of the algorithm, which does not incur in outliers even for large perturbations. This depends on the fact that D is included among the estimated variables. In this case, the EKF initializes the estimate $\hat{D}_0$ of D with its nominal value $D_n = 1$ m, while, in each simulation, the real D is generated according to $D = D_n + n_D$, with $n_D \sim \mathcal{N}(0, \sigma_D)$. When σ_D is very small (e.g., $\sigma_D = 0.01$ m in Table IV), we could not use this value in the EKF (namely, in Eq. (11)), but we should also take into account the uncertainty related to the unknown offset. In fact, as mentioned, the estimate of D compensates the effect of the unknown offset, which ranges uniformly in $(0, \pi)$. This roughly corresponds, in the measurement setup considered in this paper, to a uniform metric uncertainty of about 0.09 m. This additional uncertainty can be modeled by a Gaussian random variable with standard deviation 0.02 m. Since the uncertainty in the knowledge of D and in the offset are independent, the standard deviation to be considered in the EKF is $\sqrt{\sigma_D^2 + 0.02^2}$. This value, however, roughly coincides with σ_D when σ_D is large enough (e.g., in Table IV, when $\sigma_D \geq 0.05$).

Finally, in Table V, we report the effect of the Gaussian noise n_ϕ in the phase measurements. It is possible to see that a satisfactory performance can be obtained if σ_ϕ is not larger than 15° while, for $\sigma_\phi = 20°$, the estimation error significantly increases and 35 outliers (out of 1000 simulations) have been observed.

V. EXPERIMENTAL RESULTS

The proposed approach has been applied to a real data set, where the measurements have been taken in a situation

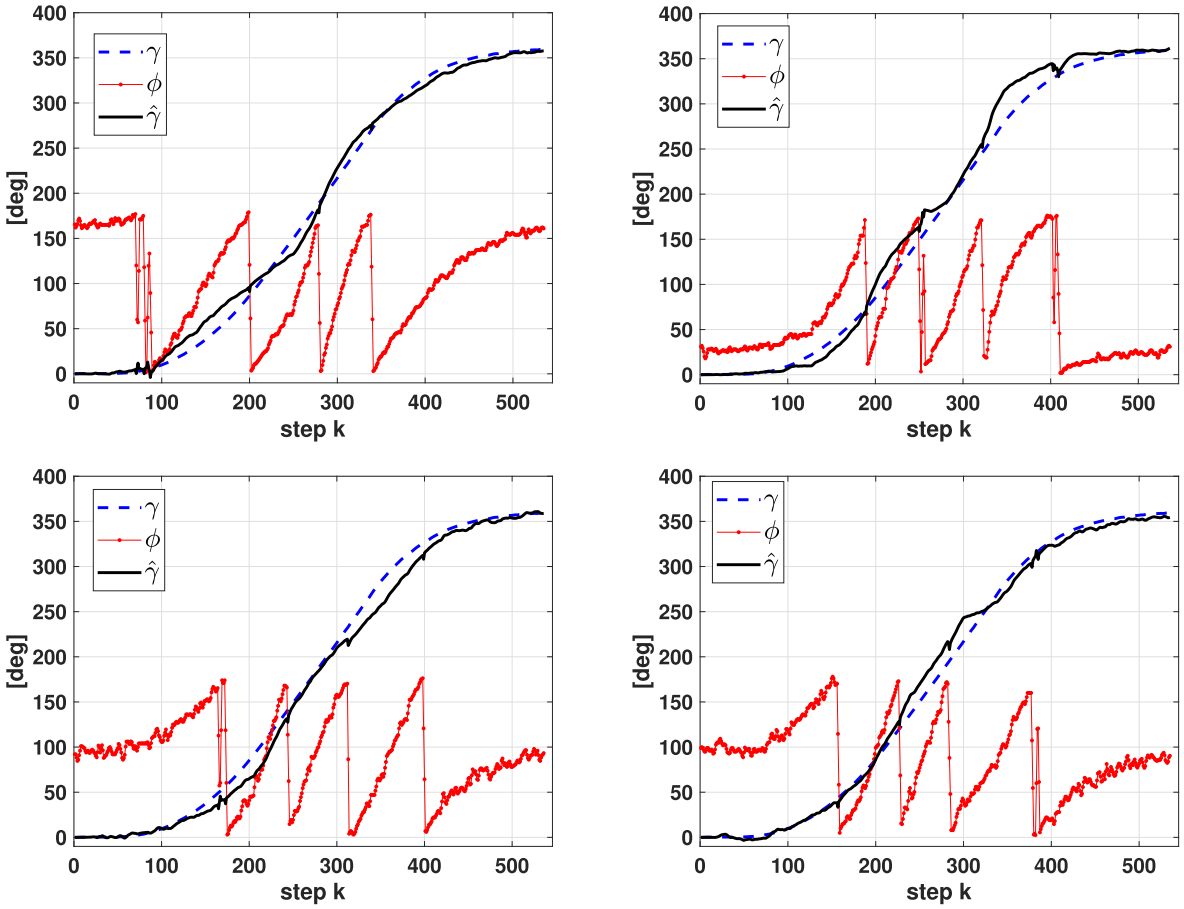

Fig. 6. The algorithm applied in the experimental setup described in Section V: the rotation angle γ and its estimate $\hat{\gamma}$ are reported together with the phase measurements. The average estimation errors e_γ obtained in the different experiments are 7.49° (top-left), 9.91° (top-right), 8.51° (bottom-left) and 6.61° (bottom-right).

similar to the perturbed scenario described in Section IV-B. As mentioned in that section, the EKF has been executed with the nominal value of the unknown parameters (in this case $D_n = 2.5$ m, $AR = 1$, $r_{0x} = r_{0y} = r_c = 0$), assuming a relatively large standard deviation $\sigma_\phi = 60°$ characterizing the noise in the phase measurements. We performed an offline execution of the EKF where samples are assumed to arrive in every time unit (i.e., $\delta_T = 1$) and, based on the small observed change in the rotation speed, we assigned in the EKF $\sigma_\tau = \sigma_{\alpha,0} = 0.87 \cdot 10^{-5} deg/s^2$. In all the experiments we considered a 360° rotation. The reader and the tag were only approximately positioned according to the nominal setup and, even if the true value of the different unknown parameters was not measured during the experiments, we expect significantly large deviations of D, AR, r_{0x}, r_{0y} and r_c from their nominal value (e.g., in the order of 1 m for r_{0x} and r_{0y} and in the order of 0.1 m for D and r_c).

The measurement set-up is composed of an Me6 ThingMagic reader equipped with an RHCP antenna having maximum gain 6dB and operating frequency 867MHz. The reader is installed onboard a unicycle like robot (see Fig. 7). The tag, positioned on the ceiling of the environment, is a dipole-like antenna LabID UH107 anchored to a metallic plane by means of a quarter wavelength thick styrofoam slab. The ceiling height is about 2.5 m. This is, as mentioned, the nominal value assigned to the D coordinate (i.e., $D_n = 2.5$ m). During the experiments, the robot performed a rotation around its center, only approximately positioned on the projection of the tag on the floor and slightly different in each experiment (that is, the robot was moved between the experiments). The ground truth of the rotation was obtained through two rotary incremental optical encoders with 2-bit Gray Code, mounted on the actuated wheels of the robot. The encoders are characterized by a resolution of 12 pulses per rotation. Due to the connecting gears and to other robot parameters (such as the radius and the track of the wheels), we obtained about 500 encoder pulses for a 360° robot rotation.

We report in Fig. 6 the performance obtained in 4 different experiments. According to the figure, it is possible to see how the average estimation error obtained in these experimental tests is always less than 10°.

VI. Conclusion

The dependence of the phase of the backscattered RFID signal on the relative orientation between the tag's and the reader's antennas, occurring in some configuration scenarios, has been often considered as a disturbance in some localization

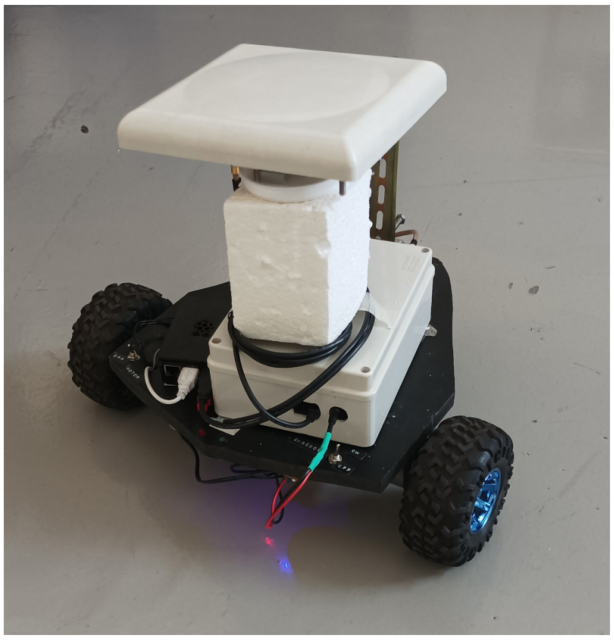

Fig. 7. The experimental setup: the Me6 ThingMagic reader is mounted on a unicycle robot with two actuated wheels with rotary incremental optical encoders. The center of the antenna approximately matches with the robot center of rotation.

contexts. In this paper, on the contrary, it has been regarded as an interesting feature which allows to estimate the orientation of a tagged object through a simple procedure based on off-the-shelf components.

The reader is equipped with a circularly polarized RFID antenna and is positioned in front of the rotating object (with a linearly polarized tag) at a certain nominal distance, only roughly known.

An Extended Kalman filter, only using the phase measurements as inputs (together with a rough knowledge on the maximum rotation acceleration), is designed according to a nominal configuration setup and estimates the rotation angle, velocity and acceleration together with the tag-reader distance. As explained in the paper, the tag-reader distance is included among the estimated variables since its effect on the phase measurements is particularly relevant and also because its estimation allows to compensate the error associated with the lack of the knowledge on the phase measurement offset. The effect of other uncertain parameters is less relevant and for this reason they are not included among the EKF variables: this allows to reduce the computational complexity of the filter and also to improve its convergence chance.

A numerical investigation has been reported in the paper to show that the proposed system is robust with respect to the uncertainty in the unknown parameters and this allows to obtain satisfactory results in experimental contexts, where the nominal configuration setup can only approximately be reproduced.

The proposed method is suitable for many practical applications where the measurement of the rotation speed or the angular variation is required. It is a valid alternative, especially in harsh environments, to other methods based on different technologies. A limit to the maximum measurable speed is due to the interrogation rate of the reader as well as to the noise.

REFERENCES

[1] K. Zannas, H. E. Matbouly, Y. Duroc, and S. Tedjini, "From identification to sensing: Augmented RFID tags," *Wireless Power Transmission for Sustainable Electronics*. Hoboken, NJ, USA: Wiley, 2020, pp. 223–246.

[2] C. Li, L. Mo, and D. Zhang, "Review on UHF RFID localization methods," *IEEE J. Radio Freq. Identification*, vol. 3, no. 4, pp. 205–215, Dec. 2019.

[3] M. Le Breton, F. Liébault, L. Baillet, A. Charléty, É. Larose, and S. Tedjini, "Dense and long-term monitoring of earth surface processes with passive RFID—A review," *Earth Sci. Rev.*, vol. 234, Nov. 2022, Art. no. 104225.

[4] X. He, J. Zhu, W. Su, and M. M. Tentzeris, "RFID based non-contact human activity detection exploiting cross polarization," *IEEE Access*, vol. 8, pp. 46585–46595, 2020.

[5] E. DiGiampaolo and F. Martinelli, "A multiple baseline approach to face multipath," *IEEE J. Radio Freq. Identification*, vol. 4, no. 4, pp. 314–321, Dec. 2020.

[6] P. Yang, Y. Feng, J. Xiong, Z. Chen, and X.-Y. Li, "RF-ear: Contactless multi-device vibration sensing and identification using COTS RFID," in *Proc. IEEE Conf. Comput. Commun. (IEEE INFOCOM)*, 2020, pp. 297–306.

[7] M. Le Breton, É. Larose, L. Baillet, Y. Lejeune, and A. van Herwijnen, *Monitoring Snowpack SWE and Temperature Using RFID Tags As Wireless Sensors*. Munich, Germany: EGUsphere, 2022, pp. 1–24.

[8] G. Gupta, B. P. Singh, A. Bal, D. Kedia, and A. Harish, "Orientation detection using passive UHF RFID technology [education column]," *IEEE Antennas Propag. Mag.*, vol. 56, no. 6, pp. 221–237, Dec. 2014.

[9] E. DiGiampaolo, F. Martinelli, and F. Romanelli, "Considering polarization mismatch in modeling the RFID phase offset variability for tag localization," in *Proc. IEEE 12th Int. Conf. RFID Technol. Appl. (RFID-TA)*, 2022, pp. 21–24.

[10] Y. S. Didosyan, H. Hauser, H. Wolfmayr, J. Nicolics, and P. Fulmek, "Magneto-optical rotational speed sensor," *Sensors Actuators A Phys.*, vol. 106, nos. 1–3, pp. 168–171, 2003.

[11] H.-J. Sheng et al., "Random rotary position sensor based on fiber Bragg gratings," *IEEE Sensors J.*, vol. 12, no. 5, pp. 1436–1441, May 2012.

[12] T. Addabbo et al., "Instantaneous rotation speed measurement system based on variable reluctance sensors for torsional vibration monitoring," *IEEE Trans. Instrum. Meas.*, vol. 68, no. 7, pp. 2363–2373, Jul. 2019.

[13] X. Liu, C. Liu, and P. W. Pong, "Velocity measurement technique for permanent magnet synchronous motors through external stray magnetic field sensing," *IEEE Sensors J.*, vol. 18, no. 10, pp. 4013–4021, May 2018.

[14] Y. Zhou, L. Dong, C. Zhang, L. Wang, and Q. Huang, "Rotational speed measurement based on LC wireless sensors," *Sensors*, vol. 21, no. 23, p. 8055, 2021.

[15] P. Paramo-Balsa, J. M. Roldan-Fernandez, F. Gonzalez-Longatt, and M. Burgos-Payan, "Measurement of the speed of induction motors based on vibration with a smartphone," *Appl. Sci.*, vol. 12, no. 7, p. 3371, 2022.

[16] F. Natili, F. Castellani, D. Astolfi, and M. Becchetti, "Video-tachometer methodology for wind turbine rotor speed measurement," *Sensors*, vol. 20, no. 24, p. 7314, 2020.

Emidio Di Giampaolo received the Laurea degree in electronic engineering and the Ph.D. degree in applied electromagnetics from the University of L'Aquila, Italy, in 1994 and 1998, respectively.

Since 1998 to 2004, he has been Postdoctoral Researcher with the University of L'Aquila. In the Spring of 2000, he was a Visiting Researcher with the European Space Research and Technology Centre, Noordwijk. From 2005 to 2009, he was a Researcher with the University of Rome Tor Vergata. Since 2010, he has been with the University of L'Aquila as an Associate Professor. His research interests mainly concern numerical methods for modeling radio-wave propagation in complex environments, antennas, and radio localization.

Francesco Martinelli was born in Rome, Italy, in 1969. He received the Laurea degree (cum laude) in electrical engineering and the Ph.D. degree in computer science and automation engineering from the University of Rome Tor Vergata, Italy, in 1994 and 1998.

He is currently an Associate Professor with the University of Rome Tor Vergata. In 1997, he was a Visiting Scholar with the Department of Manufacturing Engineering, Boston University, Boston, MA, USA. His research interests include mobile robot localization, dynamic scheduling of manufacturing systems, and filtering methods.

Fabrizio Romanelli (Graduate Student Member, IEEE) was born in Viterbo, Italy, in 1979. He received the B.S. and M.S. degrees in automation engineering from the University of Rome Tor Vergata in 2005, where he is currently pursuing the Ph.D. degree in computer science, control and geoinformation, University of Rome Tor Vergata focusing on robotic perception and sensor fusion techniques.

From 2006 to 2017, he was a Robotics Specialist and a Software Manager with the Research and Development Department, Comau Robotics S.p.A., Turin, Italy. From 2017 to 2019, he was a Research Engineer with the Istituto Italiano di Tecnologia, Genoa, Italy, in the Advanced Robotics Research Line designing the software architecture for legged robots. He is the author of 14 articles and 1 book chapter. He was the finalist at EUROP/EURON Technology Transfer Award 2009 and won the second prize at EUnited Robotics Technology Award 2014. He holds two patents. His research interests include resilient robotic perception, sensor fusion techniques, simultaneous localization and mapping, visual SLAM and gyrotrons management and remote control for Tokamak divertor.

Open Access funding provided by 'Università degli Studi di Roma "Tor Vergata"' within the CRUI CARE Agreement